Effects of potassium on the adsorption of methanol on β-Mo$_2$C(001) surface

C. Pistonesi [a], A. Juan [a,*], A.P. Farkas [b], F. Solymosi [b]

[a] Departamento de Física, Universidad Nacional del Sur, Avda. Alem 1253, 8000 Bahía Blanca, Argentina
[b] Reaction Kinetics Research Group, Chemical Research Centre of the Hungarian Academy of Sciences, University of Szeged, P.O. Box 168, H-6701 Szeged, Hungary

ARTICLE INFO

ABSTRACT

We have studied the effect of K on the adsorption of methanol on the β-Mo$_2$C(001) surface and compared our experimental data with theoretical calculations. We have also performed high resolution electron energy loss spectroscopy (HREELS) (LK, ELS3000). For calculations we used the density functional theory under the VASP implementation. The most favorable sites for methanol adsorption are on top of a Mo atom in the clean surface and on top of a K atom in the pre-dosed surface. The changes in the work function fit our model as the surface withdraws charge from the adsorbate. The changes in the computed vibrational frequencies also agree with the HREELS results at very low coverage. The C–O bond distance increases while the O–H bond decreases making a C–O bond breakage a possibility on K covered surfaces.

1. Introduction

It has long been documented that early transition metal carbides have catalytic properties similar to the Pt group metals [1,2]. Nevertheless, recent studies revealed that certain carbides exhibit a unique catalytic property not experienced on metal surfaces. Deposition of Mo$_2$C on ZSM-5 catalyzed the aromatization of methane with high selectivity, 80–85%, at a conversion of 10–12% [3–5]. This behavior of Mo$_2$C/ZSM-5 also appeared in the aromatization of ethanol [6], methanol [7] and dimethyl ether [8]. Interestingly, when ZSM-5 was replaced with carbon support, then the reaction pathway of these compounds changed, and the production of hydrogen became prominent [9–11]. An important feature of Mo$_2$C catalyst in these reactions is its high thermal stability and long life. The catalytic activity of Mo$_2$C is further improved by adding potassium to Mo$_2$C, which considerably enhances the rate and the yield of the hydrogen formation [12].

To obtain more information on the surface processes occurring on the catalysts, the interaction of alcohols with Mo$_2$C/Mo(100) surfaces has been investigated in UHV with several electron spectroscopic methods [13]. The adsorption and dissociation of methanol on β-Mo$_2$C (001) model has been also examined with density functional theory calculations, which confirmed the experimental data and provided a deeper insight on the adsorption site and mechanism of methanol decomposition [14].

In the present work, the adsorption of methanol on potassium promoted β-Mo$_2$C(001) surface is computed using DFT calculations and the theoretical results are combined with some new HREEL spectroscopic measurements. The effect of potassium on the surface reactions of methanol and ethanol was previously reported on Ru(001) [15,16], Rh(111) [17], Pd(100) [18] and Pd/SiO$_2$ [19] surfaces. The surface properties of the clean Mo$_2$C and the effect of K deposition have been theoretically examined by Piskorz et al. [20] and by Kotarba et al. [21], respectively.

2. Computational method

All calculations were carried out employing a periodic implementation of the Kohn–Sham formalism of the density functional theory (DFT). The results presented in this paper were obtained with self-consistent DFT calculations using the Vienna Ab Initio Simulation Package (VASP) [22]. This package uses a plane-wave basis and a periodic supercell method. Potentials within the projector-augmeteted wave method (PAW) [23] and the generalized gradient approximation (GGA) with Perdew–Burke–Ernzerhof functional (PBE) [24,25] were used. For bulk optimization, the lattice parameters for β-Mo$_2$C were determined by minimizing the total energy of the unit cell using a conjugated-gradient algorithm to relax the ions [26]. A 5×5×5 Monkhorst–Pack k-point grid for sampling the Brillouin zone was considered. Larger sets of k-points were selected (6×6×6 and 7×7×7) making sure that there be no significant change in the calculated energies.

The surface was modeled by four layers slabs separated by vacuum using the DFT lattice parameters previously obtained from bulk optimization. During optimization the first two layers were allowed to

* Corresponding author. Tel./fax: +54 291 4595142.
E-mail address: cajuan@uns.edu.ar (A. Juan).

fully relax and a set of $3 \times 3 \times 1$ Monkhorst–Pack k-point set was used. Besides, for adsorption calculations the adsorbed species and the first two surface layers were allowed to relax. In all cases, the cutoff energy used was 750 eV.

The adsorption energy was computed by subtracting the energies of the gas phase species and the surface from the energy of the adsorbed system as follows:

$$E_{ads} = E(adsorbate / slab) - E(adsorbate) - E(slab)$$

From this definition, a negative adsorption energy corresponds to a stable adsorption on the surface.

Vibrational properties of methanol were calculated applying the finite-difference method to create the Hessian matrix; namely, a matrix of the second derivatives of the energy with respect to the atomic positions, diagonalized to obtain the characteristic frequencies of the system.

To understand possible charge transfer, it is useful to apportion the total charge among the different atoms in the unit cell. This can be done in various ways. One accepted technique is to calculate the charge in spheres centered at the atom positions. For binary system, there is no unambiguous way to define the integration radii and several choices are possible. In all cases, the sum of the volume of the spheres should be close to the total volume of the cell. The volume charges for the Mo_2C slab were computed using the bulk values as a reference. For a valid charge transfer comparison, we have to use the same integration radii in the adsorbed and isolated methanol. Followig this procedure, the computed value for the atomic charges in isolated methanol present a 1% discrepancy.

For a qualitative study on bonding the concept of overlap population (OP) as implemented in the YAeHMOP code [27] was employed. For this purpose, the optimized geometries previously obtained from DFT were used. A similar procedure was implemented by Papoian et al. [28].

3. Experimental section

The details of the experiments have been described in our previous paper [13]. Briefly, the chamber was equipped with facilities for Auger electron spectroscopy (AES), high resolution electron energy loss spectroscopy (HREELS) (LK, ELS3000) and temperature programmed desorption (TPD). The HREEL spectra reported here were acquired with a primary beam energy of 6.5 eV. Angles of incidence and reflection were 60° with respect to the surface, normal in the specular direction. The Mo(100) crystal used in this work was supplied by Materials Research Corporation — purity 99.99%. Initially the sample was cleaned by cycled heating in oxygen. This was followed by cycled argon ion bombardment (typically 1–2 kV, 1×10^{-7} mbar Ar, 10 µA for 10–30 min), and annealing at 1270 K for several minutes. The Mo_2C over Mo(100) surface was prepared by the method developed by Schöberl [29]. The Mo(100) surface was exposed to 200 L of ethylene at 900 K and then flashed to 1200 K in UHV. The resulting surface showed the characteristic three-lobe line shape of carbidic carbon in AES at 255.6, 262.1 and 272.7 eV. The $Mo_2C/Mo(100)$ sample prepared in this way was previously examined by XPS. The binding energies at 227.5–228.2 eV and 230.7–231.05 eV for $Mo(3d_{5/2})$ and $Mo(3d_{3/2})$ and 283.0 eV for C(1s) correspond closely to the values of Mo_2C [30–32]. Methanol was supplied by Scharlau Chemie — 99.98%, and was cleaned by several freeze-pump–thaw cycles. A commercial SAES getter source situated 3 cm from the sample was used to deposit potassium metal onto the Mo_2C surface. The onset of potassium desorption from the second adlayer ($Tp = 355$ K) was accepted as an indication of the completion of a monolayer denoted by $\Theta_K = 1.0$ ML. Based on LEED measurements the potassium coverage at 1.0 ML related to the underlying unit cell was estimated to be ~0.33 in the case of Pt metals [33]. This value on $Mo_2C/Mo(100)$ surface has not been determined yet.

4. Results

4.1. Bulk and surface characterization

4.1.1. Bulk properties

We first tested the parameterization of the DFT method (cutoff energy value, k-point set, smearing function, etc) for the description of the bulk β-Mo_2C. The β-Mo_2C phase has an orthorhombic crystal structure with Mo atoms slightly distorted from their positions in close-packed planes and carbon atoms occupying one-half of the octahedral interstitial sites. Thus, many reports refer to the (0001) plane as a closest-packed surface. The corresponding unit cell is composed by eight molybdenum atoms and four carbon atoms.

The calculated DFT lattice parameters for the bulk β-Mo_2C are $a = 5.273$ Å, $b = 6.029$ Å, $c = 4.775$ Å, which are very close to the experimental values ($a = 5.195$ Å, $b = 6.022$ Å, $c = 4.725$ Å) [34]. Our computed value for the bulk modulus was 307.1 Gpa, in excellent agreement with the experimental data of 307 GPa [35]. Each of the lattice parameters were overestimated in 1–2%. The bulk β-Mo_2C lattice parameters were determined for later use in investigations of supercell properties described in the next section.

4.1.2. Surface properties

The structure of β-Mo_2C (001) surface includes a series of alternating Mo and C layers. We modeled the surface with a slab of four layer thickness (two layers of Mo atoms and two layers of C atoms) and each slab has two formula unit cells width. The vacuum spacing between two repeated slabs was 11.8 Å to ensure no significant interaction between the slabs. During optimization, surface Mo and subsurface C layers were allowed to fully relax, while the other two layers were frozen at their bulk lattice parameters. The resulting interlayer distances become shorter than those in the bulk. Due to the surface discontinuity, the broken bonds make a layer constriction of 17%. This is a common effect usually reported in the literature [21].

A low potassium coverage was added on the surface on three fold positions. Although similar adsorption energies were obtained at different adsorption sites, a preferential tri-coordinated model at low coverage was obtained on similar systems [36,37]. For this system, surface Mo and subsurface C layers, and also K atom were allowed to fully relax during optimization.

We considered a K coverage of 1/8, defined as the ratio between the number of adsorbed K atoms and surface Mo atoms. The optimized K–Mo distance was 3.6 Å (see Fig. 1). A similar K-metal distance of 3.5 Å was obtained by Calzado et al. [36] for K adsorption on tri-coordinated $TiO_2(110)$ surface.

Regarding the electronic structure, surface Mo atoms showed an increase in the electron density of about 0.02 e− on its charge, while K resulted positively charged. Similar results were obtained by Kotarba et al. [21].

4.2. Methanol adsorption

The adsorption of the methanol molecule was investigated on clean and on potassium promoted Mo_2C surface using DFT. In all cases, the adsorbate was fully relaxed and so were the first two layers of the slab and the K adlayer.

We adsorbed methanol on the clean surface with the O atom bonded to a Mo atom on a top position and the H atom pointing towards a 3-fold position, (as reported in a previous paper [14]).

For methanol adsorption on potassium promoted Mo_2C surface, two adsorption sites were considered: bonded to a Mo atom on a top position (Mo_1, see Fig. 1), similar to the previous case; and bonded to the K atom on top. Distances and angles for isolated and adsorbed methanol for the three cases and adsorption energies are listed in Table 1. Fig. 2 shows the adsorption geometries.
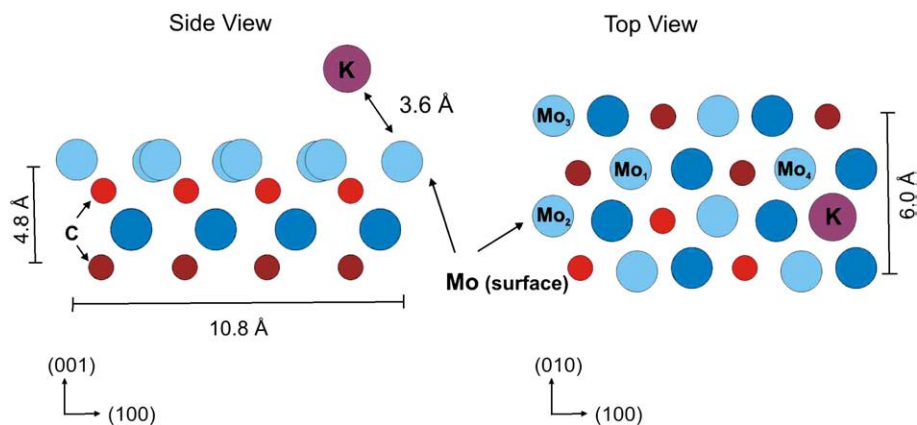
Fig. 1. Two views of the potassium promoted Mo₂C slab.

In the case of methanol adsorption on a clean surface, its O atom is bonded to a Mo atom on a top position with an O–Mo distance of 2.20 Å and with the H atom pointing towards a 3-fold position. The H–O–CH₃ angle increases by 5%, also O–H and O–C distances increase by 5% and 1% after adsorption. Similar methanol adsorption sites, bond distances and elongations were obtained by Chen et al. [38] on Au(111) surfaces and by Bakó and Pálinkás [39] on Pt(111) surfaces, both using DFT calculations.

When considering the K-promoted surface, the adsorption of methanol on a Mo top site results in a similar geometry as in the previous case although methanol is a little further from the surface (about 4%). On the other hand, on a K top site, the methanol molecule, now bonded to the K atom, is far from surface Mo atoms. The C–O distance has a small increase while O–H distance is 3% smaller when compared with methanol adsorbed on a Mo top position. Similar distances were obtained by Li et al. [40] from DFT calculations on Au₃⁺–(CH₃OH) complexes.

The computed adsorption energy for methanol on clean Mo₂C results −0.386 eV (−37.8 kJ/mol), in excellent agreement with the value of 37 kJ/mol measured from temperature programmed desorption [13]. Among these three sites, the adsorption of methanol on a K top site is more favorable than on Mo top.

Table 2 shows the computed charges for the clean surface and the methanol molecule. The surface withdraws charge from the molecule making it more negative in such a way that the molecule becomes positively charged as a whole, creating a positive outward dipole moment. A similar result was experimentally determined in the case of methanol and ethanol adsorption on Mo₂C [13,41] from changes in the work function. The increase in the electric charge on a surface Mo atom is about 3% (a decrease in the positive charge means an increase in the electron density). The first row in Table 2 shows that the electric charge on Mo₁ changes from 0.993 to 0.968, increasing 0.025 e− after

adsorption. When comparing the adsorbed specie with an isolated methanol molecule in vacuum, the H belonging to the OH group also loses some of its orbital occupation — circa 38%, reinforcing the idea of charge transfer towards the surface. The C atom presents a small reduction in its charge, while the charge of the O atom remains almost the same.

Table 3 presents the computed charges for the K-promoted surface and the methanol molecule adsorbed on the two considered sites. The charge transfer to the surface is modified and the surface becomes more negatively charged while the methanol molecule becomes more positively charged in both sites when compared with the adsorption on the clean Mo₂C surface.

The increase in the charge on surface Mo atom close to methanol is 22% after adsorption on Mo top (on K-promoted surface). The first row in Table 3, shows that the charge in Mo₁ changes from 1.008 to 0.827, increasing 0.181 e−. The comparison of methanol molecule adsorbed on Mo top shows that the main difference is in the charge in

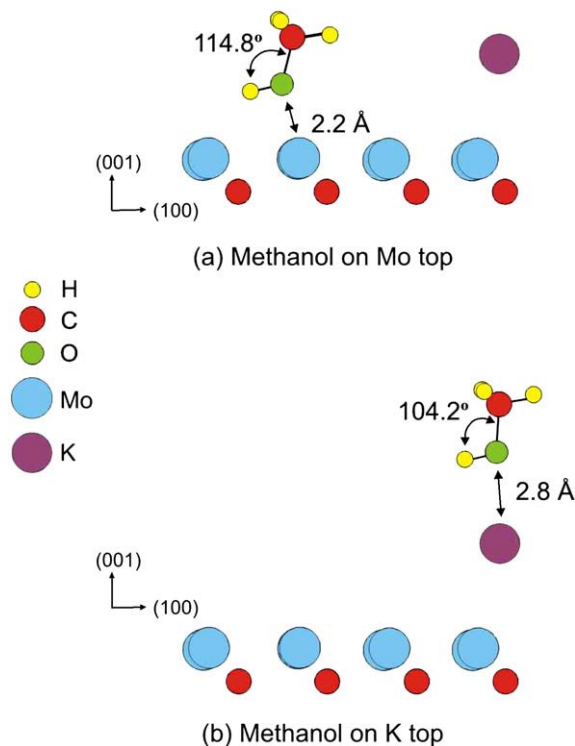**Fig. 2.** Surface structure of methanol adsorption on K–Mo₂C surface on a Mo top site (a), and on a K top site (b). For clarity, not all the surface is shown and only the first two layers are included.

Table 1
Calculated geometric parameters for isolated and adsorbed methanol. Adsorption energies are included.

		Isolated methanol	Adsorbed methanol		
			Clean Mo₂C Mo top site	K–Mo₂C Mo top site	K–Mo₂C K top site
E_{ads} (eV)		–	−0.386	−0.287	−0.388
Distance (Å)	C–O	1.42	1.43	1.43	1.45
	O–H	0.95	1.00	1.00	0.97
	O–Mo₁	–	2.20	2.28	–
	H–Mo	–	2.40	2.48	
	O–K	–	–	–	2.78
Angle (°)	COH	106.8	112.6	114.8	104.2
	CO(Mo/K)	–	159.1	154.0	176.0

Table 2
Net charges for specific atoms on Mo$_2$C surface and on isolated and adsorbed methanol.

	Isolated		Methanol on surface
	Mo$_2$C surface	Methanol	
Mo$_1$	0.993	–	0.968
Mo$_2$	0.866	–	0.852
Mo$_3$	0.989	–	0.970
Mo$_4$	0.993	–	0.992
C	− 1.252	–	− 1.283
H(CH$_3$)	–	− 0.050	− 0.040
H(OH)	–	− 0.313	− 0.195
C	–	− 1.760	− 1.704
O	–	2.352	2.348
			$\Delta q = 0.201$[a]

Atom labels are indicated in Fig. 1.
[a] The Δq is referenced to an hypothetical charge in the isolated methanol.

the H atom (from OH group) which is 8% smaller on K-promoted surface than on the clean surface.

Always comparing with the methanol molecule adsorbed on a clean surface, when methanol is adsorbed on K top site, the H atom from OH shows more electron density, the C atom presents an even greater reduction on its charge and the O atom also reduces its charge.

In the case of potassium dosed surface after methanol adsorption, we observed that potassium charge change from + 0.641 to + 0.482 when methanol is adsorbed on K top, while the charge remains almost the same (0.653) when adsorbed directly to a Mo atom. Hence, potassium is recovering some charge from the adsorbed methanol.

When methanol is adsorbed on K-promoted surface, the charge transfer to the surface is higher than in the case of adsorption on the clean surface. This happens because methanol molecule becomes more positively charged when it is adsorbed on K-promoted surface (compare Δq for methanol in the fourth column of Table 2 vs the corresponding values in the fourth and fifth columns of Table 3). Also, the increase on Mo surface charge is higher on K-promoted surface when comparing Mo charges before and after adsorption (note: compare the second column with the fourth in Table 2 and the second column with the fourth and five in Table 3).

When methanol is adsorbed on Mo top (close to K), it transfers electron density to the surface. When it is adsorbed on K top, it transfers almost the same electron density to the K atom, in the latter case, resulting in an important increase on K charge.

Table 4 shows the overlap population computed using the YAeHMOP package, commonly referred as OP, for bonds on isolated and adsorbed methanol. We can see similar behavior in the methanol adsorbed on Mo top both on clean and K-promoted surface. When

Table 3
Net charges for specific atoms on K–Mo$_2$C surface and on isolated and adsorbed methanol (on Mo top and K top sites).

	Isolated		Methanol on Mo top	Methanol on K top
	K–Mo$_2$C surface	Methanol		
Mo$_1$	1.008	–	0.827	0.840
Mo$_2$	0.849	–	0.656	0.654
Mo$_3$	1.011	–	0.819	0.831
Mo$_4$	0.974	–	0.808	0.798
K	0.641	–	0.653	0.482
H(CH$_3$)	–	− 0.050	− 0.039	− 0.040
H(OH)	–	− 0.313	− 0.179	− 0.225
C	–	− 1.760	− 1.704	− 1.667
O	–	2.352	2.354	2.367
			$\Delta q = 0.228$[a]	$\Delta q = 0.228$[a]

Atom labels are indicated in Fig. 1.
[a] The Δq is referenced to an hypothetical charge in the isolated methanol.

Table 4
Overlap population (OP) for bonds in isolated methanol and adsorbed species.[a]

OP	Isolated	On Mo$_2$C	On K–Mo$_2$C	
			Mo top	K top
C–H (from CH$_3$)	0.807	0.804	0.804	0.816
C–O	0.536	0.549	0.549	0.528
O–H	0.619	0.642	0.641	0.717

[a] Computed with YAeHMOP.

methanol is adsorbed on Mo top, the OP value for the C–O bond shows a small increase which means a small reinforcement in bond strength, whereas when adsorbed on a K top site, the C–O bond OP decreases 4%. Such bond weakening is in agreement with the increase on C–O distance.

The O–H bond presents very small bond strength reinforcement when adsorbed on Mo top, but a higher (12%) reinforcement when adsorbed on K top, which is also in agreement with the reduction on the O–H distance.

For methanol adsorbed on clean Mo$_2$C surface, the dissociation to a methoxy specie was energetically favorable, and these results supported the idea of the H abstraction from O–H group [14]. Our present results make a different dissociation mechanism possible for methanol adsorbed on K top position in which H abstraction seems not to be the most favorable process due to the O–H bond reinforcement.

Table 5 shows the calculated and experimental vibrations of methanol and its possible dissociation products. Regarding methanol adsorption on Mo top site the calculated O–H stretching frequency is 3062 cm^{-1}. This frequency has an important red shift of about 695 cm^{-1} when compared with the free molecule which is at 3757 cm^{-1}; thus, indicating the possible activation of the bond. The corresponding CO frequency has only a small reduction with a value of 1048 and 998 cm^{-1} with respect to 1079 cm^{-1} in the free molecule. This is in agreement with the small elongation of the OH and CO bond distances. Similar results were obtained by Chen et al. [38] for methanol adsorption on Au(111) and for Bakó and Pálinkás [39] for methanol on Pt(111).

When methanol is adsorbed on K top site, the theoretical C–O frequency is 961 cm^{-1}. A similar reduction in the CO frequency was obtained by Li et al. [40] on Au$_3^+$–(CH$_3$OH) systems. The OH frequency increases, as the OH distance decreases and the C–O bond elongates.

The adsorption of methanol on Mo$_2$C/Mo(100) at 100 K produced several intense vibration losses in the HREEL spectra (Fig. 3A). Losses identified on Mo$_2$C/Mo(100) at 100 K using a large exposure correspond very well to the characteristic vibration of molecularly adsorbed methanol, which are only slightly altered from the gasphase values (Table 5). The HREEL spectra for methanol on the K covered surface is shown in Fig. 3B,C. At low potassium coverage ($\theta_K = 0.3$) peaks appeared at 351, 650, 754, 1160, 1350 cm^{-1}. Feature at 3260 cm^{-1} drastically decreased (or disapearred) at low coverage (2 L) of methanol (Fig. 3B). In the light of the spectral changes our previous explanation was that metallic potassium (mainly at higher K coverage) enters a strong interaction with methanol to produce a stable potassium methoxy [13]. However in order to have a complete picture we should consider another pathway of the dissociation of methanol, which involves the rupture of C–O bond.

Comparing theoretical values for methanol on top of K versus on Mo close to K, all wavenumbers are higher on K except the C–O frequency which decreases from 998 to 961 cm^{-1}. The latter can be interpreted as a weakening of the C–O bond, making the presence of an O–H bond on the surface and a breakage of the C–O bond probable. In addition, the computed frequencies for the O–H bond are 3708 and 3062 cm^{-1} which indicates a stronger bond on the K top site (see theoretical values in Table 5). These results lead us to consider a different mechanism for methanol reaction on the potassium
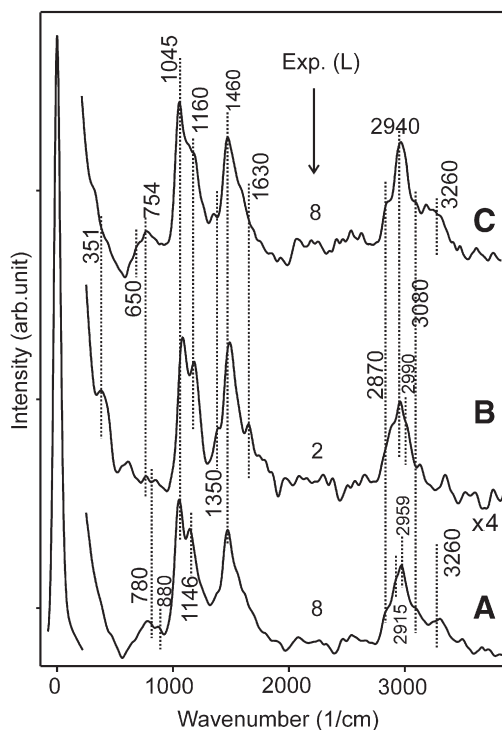
Table 5
Calculated and experimental vibrations (in cm^{-1}) of methanol and its possible dissociation products.

Vibrational mode	Experimental works							Theoretical works			
	CH_3OH IR gas phase	CH_3OH C/Mo(110) [42]	$CH_3O_{(a)}$ Rh(111) [43]	$CH_3O_{(a)}$ C/Mo(100) [42]	$K–CH_3O_{(a)}$ Ru(001) [16]	$CH_{3(a)}$ Rh(111) [44]	Present work 2 L CH_3OH 0.33 ML K Mo_2C/Mo(100)	Present work CH_3OH free molecule	CH_3OH on Pt(111) [39]	Present work CH_3OH on Mo top	Present work CH_3OH on K top
$\delta(OH)$	3681	3261						3757	3564	3062	3708
$\nu(C–H)$			2935				2990, 3080				
$\nu_a(CH_3)$	3000	2929		2936	2900	2920	2940	3061, 2996	3105	3023, 3098	3052, 3122
$\nu_s(CH_3)$	2844				2780		2870	2937	3061	2972	3003
$\delta(CH_3)$, $\delta(C–H)$	1477	1468	1450	1441	1450		1460	1465	1452	1447, 1452	1455, 1465
$\delta_a(CH_3)$	1455				1360	1350	1350	1452, 1432	1418, 1436	1412	1374
$\gamma(CH_3)$, $\rho(COH)$		1136		1150				1349, 1146	1297	1227	
$\delta_s(CH_3)$, $\rho(HCO)$						1185	1160		1134	1131	1134
$\rho(CH_3)$, $\rho(C–H)$, $\nu(CO)$,			1130								
$\nu(CO)+\rho(COH)$	1033	1028	1015	1021	1050		1045	1004	1052	1048	1071
$\nu(CO)$, $\gamma_s(CO)$									976	998	961
$\delta(OH)$, $\rho(CH_3)$,		771						1079			
$\rho(CH_2)$						760	754				
$\delta(M–OCH_3)$, (M—O)			645						545		
$\nu(M–OCH_3)$			345		390		351				
$\nu(K–OCH_3)$					180						

promoted surface when compared with the clean surface. That is, the surface chemical reaction could include H abstraction from O–H on clean Mo_2C and C–O bond breakage on K covered surface. Our experimental data fit this idea considering the vibration frequencies appearing at 754, 1160 and 1350 cm^{-1} (see Fig. 3) which probably correspond to methyl on the surface.

The differences between the computed and the experimental frequencies are within the range of other DFT calculations, being sensitive to the particular flavor of the exchange-correlation potential used [45,46].

5. Conclusions

The adsorption of methanol on clean and potassium promoted β-Mo_2C(001) surface was computed using DFT calculations. The most favorable sites are Mo top on clean surface and K top site on K-promoted surface, both with similar adsorption energy of − 37.8 kJ/mol, which is very close to the experimental value.

The surface withdraws charge from the molecule, thus generating a positive outward dipole moment. This effect is more intense on K-promoted surface.

Calculations show an excellent agreement with previous data for methanol on β-Mo_2C and our results compare very well in the case of methanol and ethanol due to their chemical similarity.

For methanol adsorbed on a K top site, we found that the C–O distance increases and C–O frequency presents the greatest decrease when compared with the methanol adsorption on Mo top site. Also, C–O bond is weakened and O–H bond is strengthened. This suggests a hypothetical dissociating mechanism in which a C–O bond breakage on K covered surfaces could be more favorable.

Fig. 3. Effects of methanol exposure on the HREEL spectra of clean (A) and K-dosed (B and C) Mo_2C/Mo(100) ($\theta_K = 0.33$ ML) at 100 K.

References

[1] S.T. Oyama, Catal. Today, 15, 1992, p. 179;
    S.T. Oyama (Ed.), The Chemistry of Transition Metal Carbides and Nitrides, Blackie Academia and Professional, Warsaw, Poland, 1996.
[2] H.H. Hwu, J.G. Chen, Chem. Rev. 105 (2005) 185.
[3] F. Solymosi, J. Cserényi, A. Szőke, T. Bánsági, A. Oszkó, J. Catal. 165 (1997) 150.
[4] D.W. Wang, J.H. Lunsford, M.P. Rosynek, J. Catal. 169 (1997) 347.
[5] D. Ma, Y.Y. Shu, M.J. Cheng, X.D. Xu, X.H. Bao, J. Catal. 194 (2000) 105.
[6] R. Barthos, A. Széchenyi, F. Solymosi, J. Phys. Chem. B 110 (2006) 21,816.

[7] R. Barthos, T. Bánsági, T. Süli Zakar, F. Solymosi, J. Catal. 247 (2007) 368.
[8] A. Kecskeméti, R. Barthos, F. Solymosi, J. Catal. 258 (2008) 111.
[9] R. Barthos, A. Széchenyi, Á. Koós, F. Solymosi, App. Catal. A Gen. 327 (2007) 95.
[10] R. Barthos, F. Solymosi, J. Catal. 249 (2007) 289.
[11] F. Solymosi, R. Barthos, A. Kecskeméti, Appl. Catal. A Gen. 350 (2008) 30.
[12] Á. Koós, R. Barthos, F. Solymosi, J. Phys. Chem. C 112 (2008) 2607.
[13] A.P. Farkas, F. Solymosi, Surf. Sci. 602 (2008) 1475.
[14] C. Pistonesi, A. Juan, A.P. Farkas, F. Solymosi, Surf. Sci. 602 (2008) 2206.
[15] J. Hrbek, R. De Paola, F.M. Hoffmann, Surf. Sci. 166 (1986) 361.
[16] R.A. DePaola, J. Hrbek, F.M. Hoffmann, Surf. Sci. 169 (1986) L348.
[17] A. Berkó, T.I. Tarnóczi, F. Solymosi, Surf. Sci. 189/190 (1987) 238.
[18] F. Solymosi, A. Berkó, Z. Tóth, Surf. Sci. 285 (1993) 197.
[19] J. Raskó, J. Bontovics, F. Solymosi, J. Catal. 146 (1994) 22.
[20] W. Piskorz, G. Adamski, A. Kotarba, Z. Sojka, C. Sayag, G. Djéga-Mariadassou, Catal. Today 119 (2007) 39.
[21] A. Kotarba, G. Adamski, W. Piskorz, Z. Sojka, C. Sayag, G. Djéga-Mariadassou, J. Phys. Chem. B 108 (2004) 2885.
[22] hmller, http://cms.mpi.univie.ac.at/vasp/vasp/vasp.html.
[23] G. Kresse, D. Joubert, Phys. Rev. B 59 (1999) 1758.
[24] J.P. Perdew, K. Burke, M. Ernzerhof, Phys. Rev. Lett. 77 (1996) 3865.
[25] J.P. Perdew, K. Burke, M. Ernzerhof, Phys. Rev. Lett. 78 (1997) 1396.
[26] W.H. Press, B.P. Flannery, S.A. Teukolsky, W.T. Vetterling, Numerical Recipies, Cambridge University Press, New York, 1986.
[27] G. Landrum, W. Glassey, Yet Another Extended Hückel Molecular Orbital Package (YAeHMOP), Cornell University, http://yaehmop.sourceforge.net. 1997.
[28] G. Papoian, J. Norskov, R. Hoffmann, J. Am. Chem. Soc. 122 (2000) 4129.
[29] T. Schöberl, Surf. Sci. 327 (1995) 285.
[30] J.G. Chen, B. Frühberger, J. Eng Jr., B.E. Bent, J. Mol. Catal. A 131 (1998) 285.
[31] P. Delporte, C. Pham-Huu, M.J. Ledoux, Appl. Catal. A 149 (1997) 151.
[32] L. Óvári, J. Kiss, A.P. Farkas, F. Solymosi, J. Phys. Chem. B 109 (2005) 4638.
[33] H.P. Bonzel, Surf. Sci. Rep. 8 (1987) 43 and references therein.
[34] E. Parthé, V. Sadagopan, Acta Cryst. 16 (1963) 202.
[35] J. Haines, J. Léger, C. Chateau, J. Lowther, J. Phys. Condens. Matter 13 (2001) 2447.
[36] C.J. Calzado, M.A. San Miguel, J.F. Sanz, J. Phys. Chem B 103 (1999) 480.
[37] P. Mutombo, A.M. Kees, A. Berko, V. Chab Nanotechnology 17 (2006) 4112.
[38] W. Chen, S. Liu, M. Cao, Q. Yan, C. Lu, J. Mol Struct.: THEOCHEM 770 (2006) 87.
[39] I. Bakó, G. Pálinkás, Surf. Sci. 600 (2006) 3809.
[40] Y. Li, C. Yang, M. Sun, X. Li, Y. An, M. Wang, X. Ma, D. Wang, J. Phys. Chem A 113 (2009) 1353.
[41] A.P. Farkas, F. Solymosi, Surf. Sci. 601 (2007) 193.
[42] H.H. Hwu, J.G. Chen, Surf. Sci. 536 (2003) 75.
[43] C. Houtman, M.A. Barteau, Langmuir 6 (1990) 1558.
[44] J. Kiss, A. Kis, F. Solymosi, Surf. Sci. 454–456 (2000) 273.
[45] A.Y. Lozovoi, A. Alavi, J. Electroanal. Chem. 607 (2007) 140.
[46] E.E. Fileti, S. Canuto, Inter. J. Quantum Chem. 104 (2005) 808.